

# Rapid Ammonia Gas Transport Accounts for Futile Transmembrane Cycling under $\text{NH}_3/\text{NH}_4^+$ Toxicity in Plant Roots<sup>1[C][W]</sup>

Devrim Coskun, Dev T. Britto, Mingyuan Li, Alexander Becker, and Herbert J. Kronzucker\*

Department of Biological Sciences, University of Toronto, 1265 Military Trail, Toronto, Ontario, Canada M1C 1A4

Futile transmembrane  $\text{NH}_3/\text{NH}_4^+$  cycling in plant root cells, characterized by extremely rapid fluxes and high efflux to influx ratios, has been successfully linked to  $\text{NH}_3/\text{NH}_4^+$  toxicity. Surprisingly, the fundamental question of which species of the conjugate pair ( $\text{NH}_3$  or  $\text{NH}_4^+$ ) participates in such fluxes is unresolved. Using flux analyses with the short-lived radioisotope  $^{13}\text{N}$  and electrophysiological, respiratory, and histochemical measurements, we show that futile cycling in roots of barley (*Hordeum vulgare*) seedlings is predominately of the gaseous  $\text{NH}_3$  species, rather than the  $\text{NH}_4^+$  ion. Influx of  $^{13}\text{NH}_3/^{13}\text{NH}_4^+$ , which exceeded  $200 \mu\text{mol g}^{-1} \text{h}^{-1}$ , was not commensurate with membrane depolarization or increases in root respiration, suggesting electroneutral  $\text{NH}_3$  transport. Influx followed Michaelis-Menten kinetics for  $\text{NH}_3$  (but not  $\text{NH}_4^+$ ), as a function of external concentration ( $K_m = 152 \mu\text{M}$ ,  $V_{\text{max}} = 205 \mu\text{mol g}^{-1} \text{h}^{-1}$ ). Efflux of  $^{13}\text{NH}_3/^{13}\text{NH}_4^+$  responded with a nearly identical  $K_m$ . Pharmacological characterization of influx and efflux suggests mediation by aquaporins. Our study fundamentally revises the futile-cycling model by demonstrating that  $\text{NH}_3$  is the major permeating species across both plasmalemma and tonoplast of root cells under toxicity conditions.

Ammonia/ammonium ( $\text{NH}_3/\text{NH}_4^+$ ) toxicity in higher plants has resulted in crop reduction and forest decline (Pearson and Stewart, 1993; Vitousek et al., 1997; Britto and Kronzucker, 2002), biodiversity loss (Stevens et al., 2004; Bobbink et al., 2010), and species extirpation (de Graaf et al., 1998; McClean et al., 2011). These major ecological and economic problems have been aggravated by an accelerated global nitrogen (N) cycle caused primarily by the industrialized production and use of N fertilizers (Galloway et al., 2008; Gruber and Galloway, 2008). With increasing global population and demands on agricultural production, there is no sign of this trend easing: anthropogenic N fixation has reached  $210 \text{ teragrams year}^{-1}$ , an approximately 12% increase from 2005 and an approximately 1,300% rise from 150 years ago (Galloway et al., 2008; Fowler et al., 2013).

Although considerable knowledge of the causes and mechanisms of  $\text{NH}_3/\text{NH}_4^+$  toxicity has accrued in recent years, our understanding of the key processes remains rudimentary (Gerendas et al., 1997; Britto and Kronzucker, 2002). A major hypothesis is that of futile transmembrane  $\text{NH}_4^+$  cycling, which proposes a pathological inability

of root cells to restrict the primary entry of  $\text{NH}_4^+$  at high external concentrations ( $[\text{NH}_4^+]_{\text{ext}}$ ); many downstream toxicological events are contingent upon this entry (Britto et al., 2001b). In this model, a rapid, thermodynamically passive influx of  $\text{NH}_4^+$  is coupled to an active efflux of  $\text{NH}_4^+$  that is nearly as rapid, constraining normal cellular function and energetics and resulting in plant growth decline and mortality. This phenomenon is thought to occur in  $\text{NH}_4^+$ -sensitive species such as barley (*Hordeum vulgare*) and, to a lesser extent, in tolerant species such as rice (*Oryza sativa*), which can be susceptible at higher thresholds (Balkos et al., 2010; Chen et al., 2013).

Most soils are typically acidic, especially when  $[\text{NH}_4^+]$  is high (i.e. in the millimolar range; Van Breemen et al., 1982; Bobbink et al., 1998; Britto and Kronzucker, 2002), and given the pKa of 9.25 for the conjugate pair  $\text{NH}_3/\text{NH}_4^+$ ,  $[\text{NH}_3]$  is generally low (Izaurrealde et al., 1990; Weise et al., 2013). Consequently, the fluxes of  $\text{NH}_3$  have largely been considered negligible (Britto et al., 2001a; Britto and Kronzucker, 2002; Loqué and von Wirén, 2004), in contrast to  $\text{NH}_4^+$  fluxes, which are well characterized physiologically (Lee and Ayling, 1993; Wang et al., 1993a, 1993b; Kronzucker et al., 1996) and at the molecular level (Rawat et al., 1999; von Wirén et al., 2000; Ludewig et al., 2007), at least at lower concentrations. However, the transport of  $\text{NH}_3$  across membranes has received new attention in the light of evidence that some members of the aquaporin (AQP) family of transporters, a diverse and ubiquitous class of major intrinsic proteins (Maurel et al., 2008; Hove and Bhawe, 2011), can mediate  $\text{NH}_3$  fluxes in single-cell systems (Jahn et al., 2004; Holm et al., 2005; Loqué et al., 2005; Saporov et al., 2007). However, a convincing demonstration that AQPs transport  $\text{NH}_3$  in planta is currently

<sup>1</sup> This work was supported by the Natural Sciences and Engineering Research Council of Canada, the Canada Research Chair program, and the Canadian Foundation for Innovation.

\* Address correspondence to herbertk@utsc.utoronto.ca.

The author responsible for distribution of materials integral to the findings presented in this article in accordance with the policy described in the Instructions for Authors ([www.plantphysiol.org](http://www.plantphysiol.org)) is: Herbert J. Kronzucker (herbertk@utsc.utoronto.ca).

[C] Some figures in this article are displayed in color online but in black and white in the print edition.

[W] The online version of this article contains Web-only data.

[www.plantphysiol.org/cgi/doi/10.1104/pp.113.225961](http://www.plantphysiol.org/cgi/doi/10.1104/pp.113.225961)

lacking. Given the unusually high capacity of AQP-mediated fluxes relative to those of ion channels and other transporters (Kozono et al., 2002), it is possible that sizable  $\text{NH}_3$  fluxes can be conducted through AQPs, even at very low external  $\text{NH}_3$  concentration ( $[\text{NH}_3]_{\text{ext}}$ ).

Here, we have critically reexamined the hypothesis that futile cycling is composed of cationic  $\text{NH}_4^+$  fluxes across the plasmalemma, of which an active efflux mechanism accounts for energetic demands directly contributing to toxicity (Britto et al., 2001b). We present evidence for the following alternative scenario: 1) futile cycling consists mainly of the passive electro-neutral flux of the conjugate base  $\text{NH}_3$ ; 2) such fluxes rapidly span both major membrane systems in root cells (i.e. plasmalemma and tonoplast); 3) AQPs mediate such fluxes; and 4) a thermodynamic equilibrium of  $\text{NH}_3$  is established throughout the cell, resulting in hyperaccumulation of  $\text{NH}_4^+$  in the acidic vacuole. This evidence comes primarily from positron emission tracing with the short-lived radioisotope  $^{13}\text{N}$ , used to characterize the component fluxes of futile cycling at the cellular level in the model species barley. We have coupled this with  $^{42}\text{K}^+$  radiotracing, to provide comparison with a well-understood cationic flux, as well as electrophysiological, respiratory, pharmacological, and histochemical analyses.

## RESULTS

To gauge the relative contributions of  $\text{NH}_3$  and  $\text{NH}_4^+$  transport, concentration-dependent root  $\text{NH}_3/\text{NH}_4^+$  influxes and their associated plasma membrane

depolarization (change in membrane potential [ $\Delta\Delta\Psi_m$ ]) were compared with those of the macronutrient ion potassium ( $\text{K}^+$ ; Fig. 1, A–C). In these experiments, plants were grown under nontoxic conditions, using a complete nutrient medium with  $\text{K}^+$  and  $\text{NH}_4^+$  both provided at 0.1 mM (pH 6.25). Direct influx measurements with  $^{42}\text{K}^+$  and  $^{13}\text{NH}_3/^{13}\text{NH}_4^+$ , determined between 0.1 and 10 mM for each (with the other held constant at 0.1 mM), show influx of the two ions to have vastly different rates and isotherm shapes. For instance, steady-state  $\text{NH}_3/\text{NH}_4^+$  influx (i.e. measured at the growth concentrations of 0.1 mM  $\text{K}^+$  and  $\text{NH}_4^+$ ) was 11.5-fold higher than that of  $\text{K}^+$  ( $13.12 \pm 0.85$  versus  $1.26 \pm 0.06 \mu\text{mol g}^{-1} \text{h}^{-1}$ , respectively). As each substrate's concentration independently rose to 10 mM, its influx increased 4- to 5-fold, peaking with a  $\text{NH}_3/\text{NH}_4^+$  influx 13-fold higher than that of  $\text{K}^+$  (Fig. 1A). Interestingly, however, the rise in  $\text{NH}_3/\text{NH}_4^+$  influx was not commensurate with membrane depolarization, indicating that most of the influx observed was not electrogenic and supporting the idea that  $\text{NH}_3$ , not  $\text{NH}_4^+$ , is the main transported N species. The significance of this result was underscored when compared with changes in  $\Delta\Delta\Psi_m$  observed with  $\text{K}^+$ : increases in external  $\text{K}^+$  concentration resulted in up to 4-fold greater depolarization than seen with comparable changes in  $\text{NH}_3/\text{NH}_4^+$  (Fig. 1B), despite  $\text{NH}_3/\text{NH}_4^+$  influx being more than 10 times higher than  $\text{K}^+$  influx. Only at 10 mM were depolarizations of similar magnitude observed (approximately 60 mV). Figure 1C further illustrates this disproportion, by showing  $\Delta\Delta\Psi_m$  as a function of influx for each substrate. The 9-fold steeper slope with

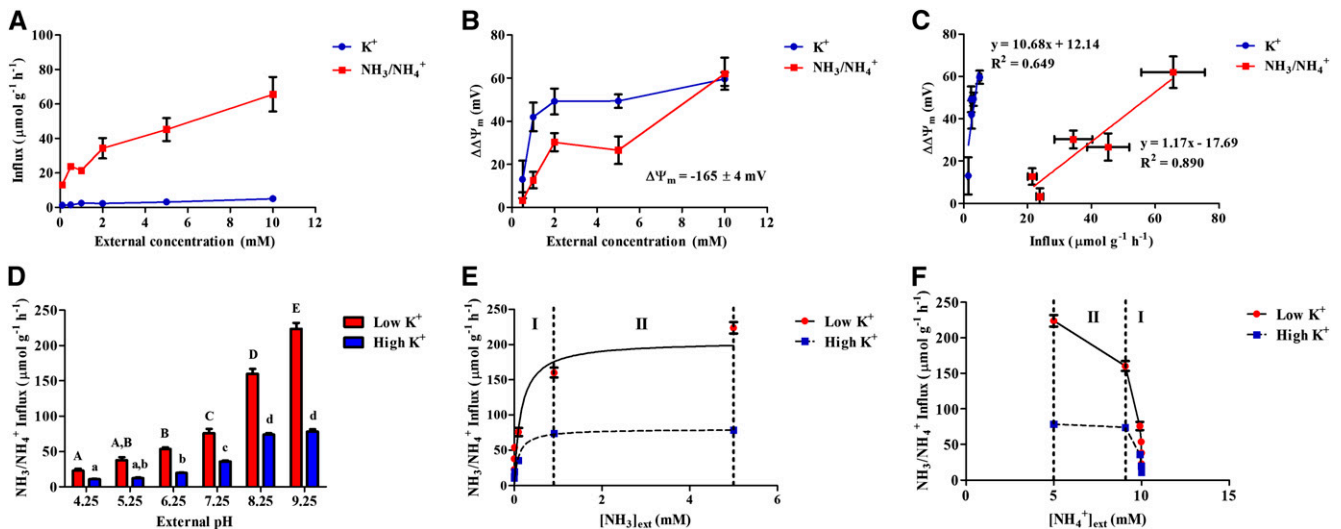


**Figure 1.**  $\text{NH}_3$  (not  $\text{NH}_4^+$ ) is the main permeating species in barley roots. A and B, Concentration dependence of influx (A) and  $\Delta\Delta\Psi_m$  (B) of  $\text{NH}_3/\text{NH}_4^+$  (red) and  $\text{K}^+$  (blue) in plants grown at 0.05 mM  $(\text{NH}_4)_2\text{SO}_4$  and  $\text{K}_2\text{SO}_4$ . C, Data from A and B replotted to show relationship between  $\Delta\Delta\Psi_m$  and influx. D, Root  $\text{NH}_3/\text{NH}_4^+$  influx as a function of external pH. E and F, Data from D replotted to show dependence of  $\text{NH}_3/\text{NH}_4^+$  influx on  $\text{NH}_3$  (E) or  $\text{NH}_4^+$  (F) concentrations, which were predicted from solution pH, according to the Henderson-Hasselbalch equation ( $\text{pK}_a$  of  $\text{NH}_3/\text{NH}_4^+ = 9.25$ ). Area I represents pH 4.25 to 8.25; area II represents pH 8.25 to 9.25. Plants were grown at 5 mM  $(\text{NH}_4)_2\text{SO}_4$  and either low (0.01 mM, red) or high (2.5 mM, blue)  $\text{K}_2\text{SO}_4$ . For all sections, error bars represent  $\pm \text{SE}$  of the mean ( $n \geq 3$ ). Letters in D denote significantly different means ( $P < 0.05$ ) as determined by a one-way ANOVA with Tukey's posthoc test. [See online article for color version of this figure.]

K<sup>+</sup> relative to NH<sub>3</sub>/NH<sub>4</sub><sup>+</sup> illustrates the much greater electrical response elicited by K<sup>+</sup> transport.

To further test the capacity of NH<sub>3</sub> transport in planta, we monitored NH<sub>3</sub>/NH<sub>4</sub><sup>+</sup> influx as a function of each conjugate species' external concentration independently, by adjusting solution pH and thus the [NH<sub>3</sub>] to [NH<sub>4</sub><sup>+</sup>] ratio (pKa = 9.25; Fig. 1, D–F). Seedlings were grown under high (10 mM) external NH<sub>3</sub>/NH<sub>4</sub><sup>+</sup> concentration ([NH<sub>3</sub>/NH<sub>4</sub><sup>+</sup>]<sub>ext</sub>) in a full-nutrient medium (pH 6.25), then placed in growth solution with pH ranging between 4.25 and 9.25 for 10 min, prior to influx measurement with <sup>13</sup>NH<sub>3</sub>/<sup>13</sup>NH<sub>4</sub><sup>+</sup>. Influx showed significant stimulations with rising pH over the entire range (Fig. 1D) and followed clear Michaelis-Menten kinetics with rising [NH<sub>3</sub>]<sub>ext</sub> (derived using the Henderson-Hasselbalch equation; Fig. 1E). By contrast, influx as a function of rising [NH<sub>4</sub><sup>+</sup>]<sub>ext</sub> showed a declining pattern, particularly above 9 mM (Fig. 1F). These effects were observed under both low (0.02 mM) and high (5 mM) external K<sup>+</sup> concentrations, which were applied in context of the known regulation of NH<sub>3</sub>/NH<sub>4</sub><sup>+</sup> fluxes by K<sup>+</sup> (Szczerba et al., 2008; Balkos et al., 2010; ten Hoopen et al., 2010). Under low K<sup>+</sup>, where NH<sub>3</sub>/NH<sub>4</sub><sup>+</sup> toxicity is most severe (Britto and Kronzucker, 2002; Balkos et al., 2010), total influx plateaued at approximately 200 μmol g<sup>-1</sup> h<sup>-1</sup>, the highest transmembrane flux of NH<sub>3</sub>/NH<sub>4</sub><sup>+</sup> hitherto reported in any plant system. Under high K<sup>+</sup>, where relief from toxicity is observed (Britto and Kronzucker, 2002), [NH<sub>3</sub>]<sub>ext</sub>-dependent influx was significantly lower, as apparent in the decrease in V<sub>max</sub> (from 204.8 ± 14.5 to 80.0 ± 4.5 μmol g<sup>-1</sup> h<sup>-1</sup> for low- and high-K<sup>+</sup> plants, respectively). By contrast, no significant differences in K<sub>m</sub> were observed between K<sup>+</sup> conditions (0.15 ± 0.05 versus 0.09 ± 0.03 mM for low- and high-K<sup>+</sup> plants, respectively). The energetic consequences of increases in NH<sub>3</sub>/NH<sub>4</sub><sup>+</sup> influx with pH were also tested using root respiration measurements. We found that, despite the much higher influx observed when pH was changed from 6.25 to 9.25, steady-state root O<sub>2</sub> consumption decreased by approximately 55% within 5 min of this change in low-K<sup>+</sup>, high-NH<sub>3</sub>/NH<sub>4</sub><sup>+</sup> plants (Fig. 2). By contrast, no such changes were observed when nitrate (NO<sub>3</sub><sup>-</sup>) was the sole N source.

As with influx, efflux of <sup>13</sup>NH<sub>3</sub>/<sup>13</sup>NH<sub>4</sub><sup>+</sup> from prelabeled roots was strongly stimulated by alkaline solution pH (and thus, higher external [NH<sub>3</sub>] to [NH<sub>4</sub><sup>+</sup>] ratios; Supplemental Fig. S1A). In plants grown on high NH<sub>3</sub>/NH<sub>4</sub><sup>+</sup> and low K<sup>+</sup>, sudden (at 8 min; Supplemental Fig. S1A, see arrow) upward shifts in external pH immediately and significantly stimulated <sup>13</sup>NH<sub>3</sub>/<sup>13</sup>NH<sub>4</sub><sup>+</sup> efflux, with greater stimulations observed at higher pH values. When tracer release was plotted as a function of the concomitant NH<sub>3</sub>/NH<sub>4</sub><sup>+</sup> influx (measured at the identical pH shift), we observed a strong linear relationship between efflux and influx (Supplemental Fig. S1B). Moreover, tracer release as a function of [NH<sub>3</sub>]<sub>ext</sub> (which we suggest may be equivalent to cytosolic [NH<sub>3</sub>]; see below) resulted in Michaelis-Menten kinetics similar to those seen with influx, having K<sub>m</sub> values ranging from 0.10 to 0.36 mM [NH<sub>3</sub>] (Supplemental Fig. S1B, inset).

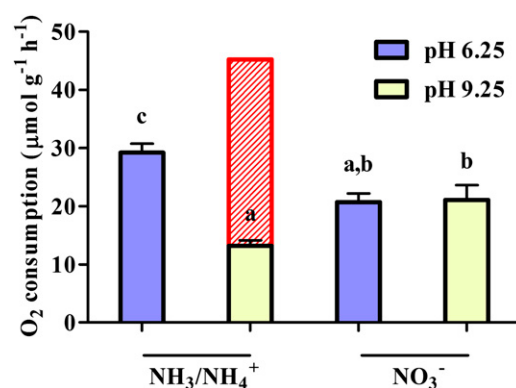


**Figure 2.** Effect of 5-min exposure to elevated pH (pH 9.25) on root respiration in barley plants grown with 0.01 mM K<sub>2</sub>SO<sub>4</sub> and 5 mM of either (NH<sub>4</sub>)<sub>2</sub>SO<sub>4</sub> or Ca(NO<sub>3</sub>)<sub>2</sub>. Red bar represents O<sub>2</sub> consumption, predicted if NH<sub>3</sub>/NH<sub>4</sub><sup>+</sup> influx at pH 9.25 is comprised entirely of cationic NH<sub>4</sub><sup>+</sup> fluxes (see Fig. 1F). Letters denote significantly different means (*P* < 0.05) as determined by one-way ANOVA with Tukey's posthoc test. [See online article for color version of this figure.]

We sought to further characterize <sup>13</sup>NH<sub>3</sub>/<sup>13</sup>NH<sub>4</sub><sup>+</sup> efflux in intact roots under toxicity conditions (low K<sup>+</sup>, high NH<sub>3</sub>/NH<sub>4</sub><sup>+</sup>) to identify the compartmental origin of tracer release (Britto and Kronzucker, 2003; Coskun et al., 2010). In roots prelabeled with tracer, <sup>13</sup>NH<sub>3</sub>/<sup>13</sup>NH<sub>4</sub><sup>+</sup> efflux was immediately suppressed by sudden (at 8 min; Fig. 3A, see arrow) exposure to 4°C or upon withdrawal of external NH<sub>3</sub>/NH<sub>4</sub><sup>+</sup>, while an external pH shift to 9.25 (from 6.25) resulted in an immediate and sizable efflux stimulation. Importantly, these findings demonstrate that efflux analysis under toxic conditions captures physiological (i.e. transmembrane) events, not artifacts of apoplastic exchange (Coskun et al., 2010, 2013). Thus, compartmental analysis by tracer efflux could be applied (Lee and Clarkson, 1986; Kronzucker et al., 1997; Britto and Kronzucker, 2003), revealing efflux to influx ratios of approximately 80% and extremely rapid rates of both unidirectional fluxes characteristic of futile cycling (Britto et al., 2001b).

Further evidence for the intracellular origin of effluxed tracer was seen in a silver (Ag<sup>+</sup>)-induced stimulation of <sup>13</sup>NH<sub>3</sub>/<sup>13</sup>NH<sub>4</sub><sup>+</sup> release (Fig. 3B). We have previously shown that sudden exposure to Ag<sup>+</sup> causes extensive damage to both major membrane systems (plasma-membrane and tonoplast) in barley roots (Coskun et al., 2012). By contrast, we observed no effect of mercury (Hg<sup>2+</sup>) application on tracer release (Fig. 3C), suggesting a lack of membrane disintegration occurring. Importantly, this qualifies the use of Hg<sup>2+</sup> as a potential inhibitor of AQPs (see below). With respect to the Ag<sup>+</sup>-induced stimulation in tracer efflux, this effect allowed for quantification of released substrate (in terms of μmol g<sup>-1</sup> root fresh weight) via integration of the <sup>13</sup>N loss and estimated intracellular specific activity, as shown previously (Coskun et al., 2012). The chemical quantity of NH<sub>3</sub>/NH<sub>4</sub><sup>+</sup> released during Ag<sup>+</sup> application (64 ± 3 μmol g<sup>-1</sup>) was very similar to that of total root tissue NH<sub>3</sub>/NH<sub>4</sub><sup>+</sup> content under control conditions, as

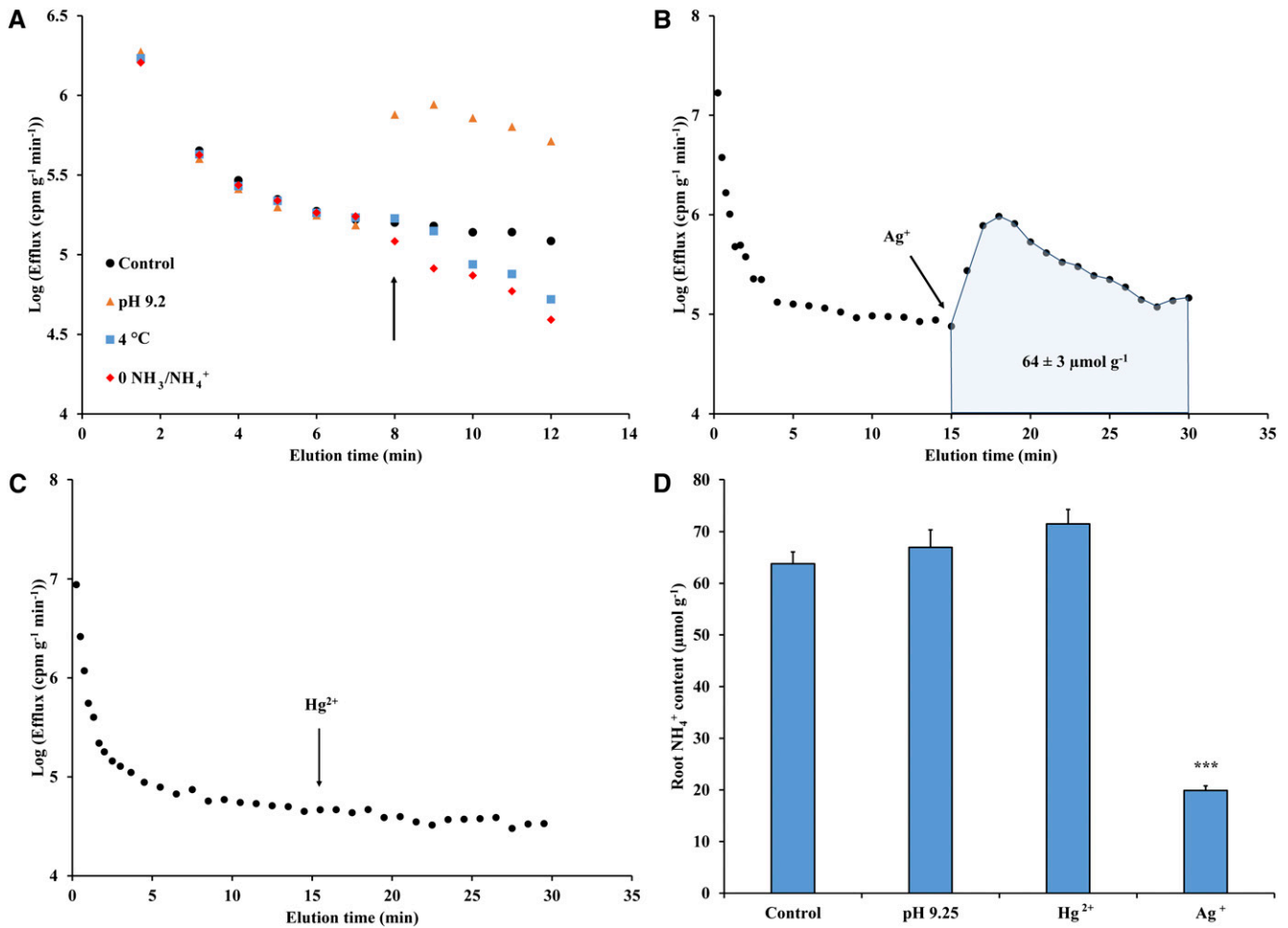


**Figure 3.** Characterization of  $\text{NH}_3/\text{NH}_4^+$  efflux from roots of intact barley seedlings. A, Effect of sudden (at 8 min; see arrow) exposure to either pH 9.25,  $4^\circ\text{C}$ , or N withdrawal from the external medium. Each point represents the mean of three to seven replicates ( $\text{SE}$  of the mean  $<15\%$  of the mean). B, Effect of sudden (at 15 min; see arrow) exposure to  $500 \mu\text{M Ag}^+$ . Integration range of tracer release due to  $\text{Ag}^+$  and results of integration are given in shaded area. Each point represents the mean of four replicates ( $\text{SE}$  of the mean  $<15\%$  of the mean). C, Lack of effect of  $500 \mu\text{M Hg}^{2+}$  application (at 15.5 min; see arrow) on root  $^{13}\text{NH}_3/^{13}\text{NH}_4^+$  efflux. Each point represents the mean of three replicates ( $\text{SE}$  of the mean  $<15\%$  of the mean). D, Root  $\text{NH}_4^+$  content measured using OPA and its effect due to 15-min exposure to pH 9.25,  $500 \mu\text{M Hg}^{2+}$ , or  $500 \mu\text{M Ag}^+$ . Each bar represents mean  $\pm \text{SE}$  of the mean ( $n \geq 6$ ). Asterisks denote significant difference from control ( $P \leq 0.001$ ) as determined by one-way ANOVA with Dunnett's posthoc test. In all sections, plants were grown at  $5 \text{ mM } (\text{NH}_4)_2\text{SO}_4$  and  $0.01 \text{ mM K}_2\text{SO}_4$ . [See online article for color version of this figure.]

measured by chemical (orthophthalaldehyde [OPA]) analysis ( $63.8 \pm 2.3 \mu\text{mol g}^{-1}$ ; Fig. 3D). We should note that, although efflux still proceeded after termination of the  $\text{Ag}^+$  treatment (Fig. 3B), the apparent premature curtailment of the treatment resulted in an underestimate of no more than approximately  $1 \mu\text{mol g}^{-1}$ , which was considered negligible. Tissue analysis (determined by OPA assay) revealed that approximately 70% of root  $\text{NH}_3/\text{NH}_4^+$  was lost during  $\text{Ag}^+$  exposure, demonstrating that the majority of cellular (i.e. both cytoplasmic and vacuolar)  $\text{NH}_3/\text{NH}_4^+$  was released (Fig. 3D). By contrast, pH 9.25 and  $\text{Hg}^{2+}$  resulted in no change in tissue  $\text{NH}_3/\text{NH}_4^+$  content (Fig. 3D), despite the significant effects on both influx and efflux of the former (see above).

Lastly, to gain mechanistic insight into  $\text{NH}_3/\text{NH}_4^+$  influx, the possible involvement of different types of

membrane transporters in  $\text{NH}_3/\text{NH}_4^+$  influx was tested by means of pharmacological profiling, in low- $\text{K}^+$ , high- $\text{NH}_3/\text{NH}_4^+$  plants (Fig. 4).  $\text{Hg}^{2+}$ , a well-known blocker of AQP activity, was applied with significant effect (36% inhibition at pH 6.25), while further support for AQP involvement was observed with treatments known to induce intracellular acidosis, which can cause closure of AQPs via protonation of conserved His residues on the cytoplasmic side (Tournaire-Roux et al., 2003; Törnroth-Horsefield et al., 2006; Ehler et al., 2009). Hydrogen peroxide ( $\text{H}_2\text{O}_2$ ) and propionic acid (PA) were two such effective treatments (30% and 54% inhibition relative to control, respectively).  $\text{N}_2$  treatment, however, was not as effective, despite its efficacy in other systems (Tournaire-Roux et al., 2003). Note that these acidifying treatments were only effective at lower external pH

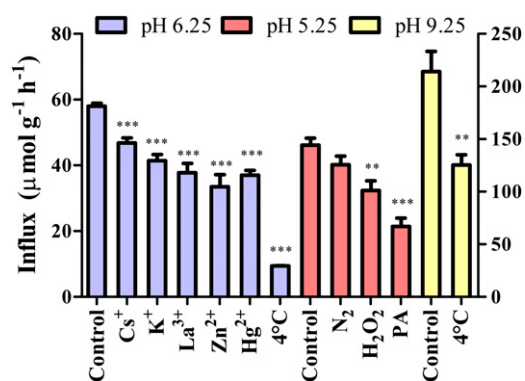


**Figure 4.** Pharmacological profile of NH<sub>3</sub>/NH<sub>4</sub><sup>+</sup> influx into roots of barley seedlings at varying external pH. Ionic inhibitors were applied as chloride salts, except for K<sup>+</sup> (applied as K<sub>2</sub>SO<sub>4</sub>). Influx at pH 9.25 corresponds to y axis on the right. Each bar represents mean ± SE of the mean (*n* ≥ 5). Asterisks denote significantly different means (\*\*, *P* ≤ 0.01; \*\*\*, *P* ≤ 0.001) from respective control, as determined by one-way ANOVA with Dunnett's posthoc test (at pH 6.25 and 5.25) or Student's *t* test (at pH 9.25). Plants were grown as in Figure 3. [See online article for color version of this figure.]

(pH 5.25). Also, Hg<sup>2+</sup> could not be tested at high pH (pH 9.25) due to hydroxide precipitation (Schuster, 1991). Other significant inhibitors of NH<sub>3</sub>/NH<sub>4</sub><sup>+</sup> influx at pH 6.25 included Cs<sup>+</sup> < K<sup>+</sup> < La<sup>3+</sup> < Zn<sup>2+</sup> << 4°C. The highest influx, seen at pH 9.25, was also suppressible at 4°C by approximately 44%.

## DISCUSSION

This study critically reexamines the nature of futile transmembrane NH<sub>3</sub>/NH<sub>4</sub><sup>+</sup> cycling in barley roots, a phenomenon with ties to NH<sub>4</sub><sup>+</sup> toxicity in a wide range of higher plants (Feng et al., 1994; Britto et al., 2001b, 2002; Chen et al., 2013). We have addressed the fundamental question of which species of the conjugate pair (NH<sub>3</sub> or NH<sub>4</sub><sup>+</sup>) is transported in the futile cycle to thus enable insight into mechanisms of transport, compartmentation, and toxicity of NH<sub>3</sub>/NH<sub>4</sub><sup>+</sup>.

The lack of agreement between ΔΔΨ<sub>m</sub> and changes in NH<sub>3</sub>/NH<sub>4</sub><sup>+</sup> influx, in contrast to K<sup>+</sup>, suggests that, above a small baseline cationic NH<sub>4</sub><sup>+</sup> flux no higher than that of K<sup>+</sup> (<5 μmol g<sup>-1</sup> h<sup>-1</sup>; Fig. 1A), electroneutral NH<sub>3</sub> transport accounts for the observed rapid rates of <sup>13</sup>N transport in intact barley roots (Fig. 1, A–C). While previous tracer studies have also demonstrated that NH<sub>3</sub>/NH<sub>4</sub><sup>+</sup> fluxes exceed those of K<sup>+</sup> at equimolar concentrations (Scherer et al., 1984; Vale et al., 1988; Wang et al., 1996), none have provided parallel membrane potential measurements. A comparison between fluxes and ΔΔΨ<sub>m</sub>, however, is of great utility in gauging the relative apportionment of NH<sub>3</sub> and NH<sub>4</sub><sup>+</sup> fluxes, as we show here.

Because such rapid NH<sub>3</sub> fluxes in planta are simply without precedent, additional investigation was called for. Further evidence in support of NH<sub>3</sub> uptake was seen in the Michaelis-Menten character of the [NH<sub>3</sub>]<sub>ext</sub>-dependent

influx isotherms (Fig. 1E). By contrast, NH<sub>4</sub><sup>+</sup> influx was seen to decline with rising [NH<sub>4</sub><sup>+</sup>]<sub>ext</sub> (Fig. 1F), ruling out a sizeable contribution from that N species. We should note, however, that because these isotherms were obtained using changes in external pH, there may be pH-specific and/or NH<sub>4</sub><sup>+</sup>-specific effects on transport. Such effects require examination, although they are inherently difficult to ascertain because pH and [NH<sub>3</sub>] to [NH<sub>4</sub><sup>+</sup>] ratios are inextricably linked. It should also be noted that in a study on rice, Wang et al. (1993b) observed a decline in <sup>13</sup>NH<sub>3</sub>/<sup>13</sup>NH<sub>4</sub><sup>+</sup> influx with rising pH at 10 mM [NH<sub>3</sub>/NH<sub>4</sub><sup>+</sup>]<sub>ext</sub>. However, the fluxes in their study were much lower than in this study and also were determined in an NH<sub>4</sub><sup>+</sup>-tolerant species. Further investigation is necessary to determine whether this is a part of the strategy by which a plant may achieve tolerance to this N source.

We also provide evidence for NH<sub>3</sub> (but not NH<sub>4</sub><sup>+</sup>) efflux under toxic (low-K<sup>+</sup>, high-NH<sub>3</sub>/NH<sub>4</sub><sup>+</sup>) conditions. Firstly, the trans-inhibition and -stimulation of efflux in response to changes in NH<sub>3</sub> provision (by substrate withdrawal and pH 9.2, respectively; Fig. 3A) suggests that NH<sub>3</sub> efflux is highly dependent on NH<sub>3</sub> influx (see also the linear dependence of the fluxes; Supplemental Fig. S1B), which is consistent with observations that efflux to influx ratios increase with rising influx (Wang et al., 1993a; Britto et al., 2002; Britto and Kronzucker, 2006). Such trans-inhibition and -stimulation of efflux have previously been shown in barley (Britto and Kronzucker, 2003) and in the mammalian literature, specifically for amino acids (White and Christensen, 1982; Sweiry et al., 1991). In the latter case, trans-stimulation of efflux has been attributed to a large counterflow through a single transporter mediating bidirectional fluxes and, as such, could in large part explain the futile NH<sub>3</sub> cycling in this paper. Further evidence that the <sup>13</sup>N efflux trace represents <sup>13</sup>NH<sub>3</sub> and not <sup>13</sup>NH<sub>4</sub><sup>+</sup> is found in its saturating response to [NH<sub>3</sub>]<sub>ext</sub> (Supplemental Fig. S1B, inset), which resembles that of influx (Fig. 1E). *K<sub>m</sub>* values for efflux, which were comparable to those for influx (ranging between 0.10–0.36 mM NH<sub>3</sub>), suggests a similar, if not identical, mechanism of NH<sub>3</sub> transport for the two fluxes. It is not clear why the efflux step should respond so readily to changes in external NH<sub>3</sub>, when substrate binding to an efflux transporter must take place intracellularly. Intriguingly, it may be that NH<sub>3</sub> transport responds to [NH<sub>3</sub>]<sub>ext</sub> in a manner that leads to a rapid equalization between NH<sub>3</sub> pools on either side of the plasma membrane, and thus NH<sub>3</sub> efflux kinetics are in fact directly responding to cytosolic [NH<sub>3</sub>] and only indirectly to [NH<sub>3</sub>]<sub>ext</sub>. NH<sub>3</sub> may shuttle rapidly among multiple cellular compartments, establishing similar equilibrium concentrations in each, where membrane permeabilities permit (see below).

The Michaelis-Menten analyses under low-K<sup>+</sup>, high-NH<sub>3</sub>/NH<sub>4</sub><sup>+</sup> conditions (see above; Fig. 1E) revealed a *V<sub>max</sub>* of about 200 μmol g<sup>-1</sup> h<sup>-1</sup> for NH<sub>3</sub> influx, the highest bona fide transmembrane flux hitherto reported in any plant system. Such rapid fluxes are orders of magnitude

higher than typical fluxes of mineral (ionic) nutrients (Britto and Kronzucker, 2006). Although fluxes of sodium ( $\text{Na}^+$ ) under toxic (saline) conditions have been reported to reach or exceed such values (Lazof and Cheeseman, 1986; Essah et al., 2003; Malagoli et al., 2008), the validity of these fluxes have recently come into question, particularly with respect to their unrealistic energetic requirements (Britto and Kronzucker, 2009; Kronzucker and Britto, 2011); moreover, such fluxes are generally reported at much higher external substrate concentrations (typically, 100 mM or higher). On the other hand, such energetic limitations do not apply to the passive electroneutral fluxes of  $\text{NH}_3$ . In fact, root  $\text{O}_2$  consumption was found to decline under such conditions (i.e. pH 9.25; Fig. 2), a result that further discounts  $\text{NH}_4^+$ -specific futile cycling, which is predicted to involve a thermodynamically active efflux (Britto et al., 2001b). Figure 2 highlights, in red, the theoretical increase in  $\text{O}_2$  consumption necessary to power an active efflux mechanism of  $\text{NH}_4^+$  when fluxes are as high as  $200 \mu\text{mol g}^{-1} \text{h}^{-1}$  based on current models of ion transport and  $\text{O}_2$  consumption (Poorter et al., 1991; Kurimoto et al., 2004; Britto and Kronzucker, 2009). This large energy deficit is consistent with the idea that futile cycling is primarily of the conjugate base,  $\text{NH}_3$ . However, unlike with the previously proposed  $\text{NH}_4^+$  cycling, the term futile here does not refer to an energy-dissipating process (e.g. Amthor, 2000), but more generally to the lack of apparent functional utility in the  $\text{NH}_3$  cycle. The fact that the pH shift did not affect root  $\text{O}_2$  consumption in  $\text{NO}_3^-$ -grown plants shows an N source specificity of this effect that will require further investigation to explain.

These results have important consequences for the compartmentation and toxicity of  $\text{NH}_3/\text{NH}_4^+$ . Compartmental analyses with  $^{13}\text{NH}_3/^{13}\text{NH}_4^+$  in roots and shoots of plants grown under toxic (high- $\text{NH}_3/\text{NH}_4^+$ ) conditions generally yield extremely high "pool sizes" of many hundred millimolar (Britto et al., 2001b, 2002), leading to the speculation that the entire cell, not simply the cytosol, acts as a single compartment of tracer origin (Britto and Kronzucker, 2003; Balkos et al., 2010). This study provides the first evidence in support of this "whole-cell" hypothesis. Because a high-capacity, thermodynamically passive  $\text{NH}_3$  transport can account for futile cycling, it is feasible that  $\text{NH}_3$  rapidly equilibrates across intracellular membranes and among cellular compartments, particularly the vacuole and cytosol (Fig. 5). How such rapid unidirectional fluxes can persist given the apparent lack of an  $\text{NH}_3$  concentration gradient across cellular compartments is an interesting question and can be most simply explained by passive diffusion through high-capacity membrane channels such as AQPs (see below). The  $\text{NH}_3$  equilibration across cellular compartments can explain why tracer accumulation (measured as counts retained in tissue or released with  $\text{Ag}^+$  application; Fig. 3B) closely agreed with that of chemical (OPA) analyses measuring tissue  $\text{NH}_3/\text{NH}_4^+$  content

(Fig. 3D). Thus, the  $\text{NH}_4^+$  content within each compartment may be ultimately determined by  $\text{NH}_3$  permeation and compartmental pH, as illustrated in Figure 5. In this revised model of futile cellular N cycling, the 0.5 to 1.5 mM range of cytosolic  $[\text{NH}_4^+]$  agrees well with measured values from studies using methods such as ion-selective microelectrodes and NMR (Lee and Ratcliffe, 1991; Wells and Miller, 2000). Importantly, the model reveals that a hyperaccumulation of  $\text{NH}_4^+$  in the vacuole would ultimately exist (Fig. 5), due to vacuolar acid trapping, and could explain the frequently observed suppressions in cationic nutrients, notably  $\text{K}^+$  (but also  $\text{Ca}^{2+}$  and  $\text{Mg}^{2+}$ ; Barker et al., 1967; Van Beusichem et al., 1988; Lang and Kaiser, 1994; Kronzucker et al., 2003), which may ultimately be the major cause of  $\text{NH}_3/\text{NH}_4^+$  toxicity in higher plants.

It is likely that the rapid  $\text{NH}_3$  cycling reported here is mediated by AQPs (Fig. 4), which have high transport capacity and are known to conduct  $\text{NH}_3$  fluxes (Jahn et al., 2004; Holm et al., 2005; Loqué et al., 2005; Saporov et al., 2007; Hove and Bhavé, 2011). Kozono et al. (2002) estimated the rate of water transport through AQP1 to be  $3 \times 10^9$  molecules per subunit per second, roughly 30-fold higher than  $\text{K}^+$  transport via the potassium crystallographically-sited activation (KcsA) channel, which is among the fastest ion channels (Morais-Cabral et al., 2001). AQP involvement is suggested by the pharmacological profiling of  $\text{NH}_3$  influx in our study, particularly in the effect of  $\text{Hg}^{2+}$ , a classic AQP inhibitor (Fig. 4). Importantly, unlike with  $\text{Ag}^+$

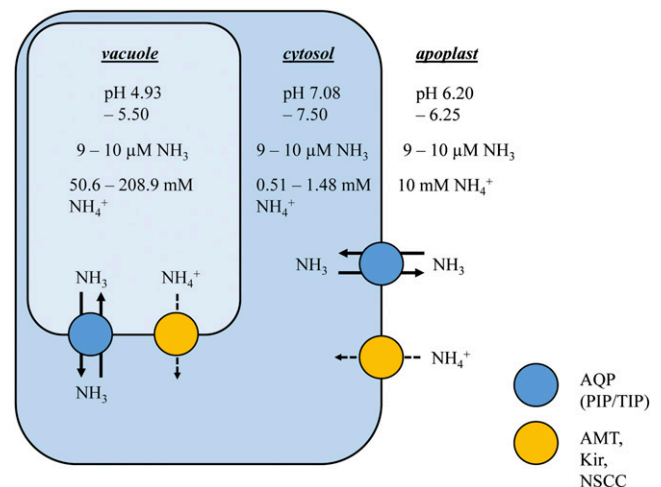


**Figure 5.** Revised model of futile transmembrane  $\text{NH}_3/\text{NH}_4^+$  cycling in root cells of higher plants. Uncharged  $\text{NH}_3$  rapidly equilibrates across both major membrane systems (plasmalemma and tonoplast) and is likely mediated by AQPs specific to each system. A relatively minor channel/carrier-mediated flux of  $\text{NH}_4^+$  may also occur across both membrane systems.  $\text{NH}_4^+$  concentrations are a function of  $\text{NH}_3$  equilibration and compartment pH (Roberts et al., 1982; Walker et al., 1996; Kosegarten et al., 1997; Kosegarten et al., 1999). PIP, Plasmalemma-intrinsic protein; TIP, tonoplast-intrinsic protein; AMT, ammonium transporter; Kir,  $\text{K}^+$  inward rectifier; NSCC, nonselective cation channel. [See online article for color version of this figure.]

(Fig. 3B), Hg<sup>2+</sup> showed no sign of causing membrane damage in our system (as manifest in lack of efflux stimulation or tissue content losses; Fig. 3, C and D; compare with Coskun et al., 2012). The strong suppressions of influx by H<sub>2</sub>O<sub>2</sub> and PA also support AQP involvement (Fig. 4; Tournaire-Roux et al., 2003; Törnroth-Horsefield et al., 2006; Ehlert et al., 2009). It is worth highlighting here, however, that pharmacological profiling, like any method, is not without its caveats. The lack of specificity of several blockers/chemical treatments (Coskun et al., 2013), as well as the need to employ relatively high concentrations at times, can potentially have secondary effects. This by no means invalidates the use of pharmacology, but highlights the importance of a diversity of experimental approaches. Future experiments with AQP antisense/knockout lines (Martre et al., 2002; Javot et al., 2003), particularly for AQPs already shown to mediate NH<sub>3</sub> fluxes (Jahn et al., 2004; Holm et al., 2005; Loqué et al., 2005), could help further elucidate their involvement in futile NH<sub>3</sub> cycling. In addition, such mutant analyses could provide a critical test of the “whole-cell distribution” hypothesis for NH<sub>3</sub> presented above (Fig. 5).

We end by highlighting the suppression of  $V_{\max}$  for NH<sub>3</sub> influx by high-plant K<sup>+</sup> status, while  $K_m$  remains unaffected (Fig. 1E). It appears that K<sup>+</sup> status has no effect on the substrate affinity of NH<sub>3</sub> transporters but regulates NH<sub>3</sub> influx by other means. One such mechanism might involve the modulation of AQP activity, which may well be expected, because, in plants, K<sup>+</sup> acquisition is the chief means of establishing osmotic balance and cell turgor (Britto and Kronzucker, 2008; Grzebisz et al., 2013). The effects of K<sup>+</sup> in the short-term suppression of NH<sub>3</sub>/NH<sub>4</sub><sup>+</sup> influx and efflux (Szczerba et al., 2008; Balkos et al., 2010; see also Fig. 4) also suggest a post-translational regulation of NH<sub>3</sub> transporters by K<sup>+</sup>. Such a mechanism may explain the agriculturally important alleviation of NH<sub>3</sub>/NH<sub>4</sub><sup>+</sup> toxicity in higher plants by K<sup>+</sup> (Barker et al., 1967; Szczerba et al., 2008; Balkos et al., 2010) and thus pave the way for future studies.

## MATERIALS AND METHODS

### Plant Culture

Barley (*Hordeum vulgare* ‘Metcalfe’) seedlings were grown hydroponically for 4 d (after 3-d germination in sand) in a climate-controlled growth chamber (Coskun et al., 2013). Hydroponic tanks contained aerated, N- and K<sup>+</sup>-free, modified Johnson’s solution (pH = 6.25) and were frequently exchanged to maintain a nutritional steady state. Depending on the experiment, N was supplied as either NH<sub>4</sub><sup>+</sup> (0.1 or 10 mM, as (NH<sub>4</sub>)<sub>2</sub>SO<sub>4</sub>) or NO<sub>3</sub><sup>-</sup> (10 mM, as Ca(NO<sub>3</sub>)<sub>2</sub>) and K<sup>+</sup> was supplied at either 0.02, 0.1, or 5 mM as K<sub>2</sub>SO<sub>4</sub> (see “Results”).

### Radiotracer Experiments

<sup>13</sup>N (half-life = 9.98 min) was used to trace the unidirectional fluxes and cellular compartmentalization of NH<sub>3</sub>/NH<sub>4</sub><sup>+</sup> in roots of intact seedlings (Kronzucker et al., 1997; Britto et al., 2001b). For steady-state influx experiments, roots were incubated for 5 min in aerated growth solution spiked with <sup>13</sup>NH<sub>3</sub>/<sup>13</sup>NH<sub>4</sub><sup>+</sup>, then desorbed in two sequential steps (for 5 s and 5 min) in nonradioactive growth solution to release tracer from extracellular spaces (Balkos et al., 2010). Treatment conditions were conducted as above, with some

modifications. These included concentration-dependent and pH-dependent isotherms, whereby growth solution [NH<sub>3</sub>/NH<sub>4</sub><sup>+</sup>]<sub>ext</sub> and pH were adjusted (with NaOH) as specified in all solutions, including a 10-min-preloading solution. Other treatments included 10 mM CsCl, 5 mM K<sub>2</sub>SO<sub>4</sub>, 10 mM LaCl<sub>3</sub>, 10 mM ZnCl<sub>2</sub>, and 500 μM HgCl<sub>2</sub>, and chilling (4°C) in preloading (10 min) and loading solutions. A subset of experiments involved a 2-h pretreatment at pH 5.25 ± N<sub>2</sub> bubbling (anoxia treatment), 2 mM H<sub>2</sub>O<sub>2</sub>, or 20 mM PA. For all treatments, after the final desorption, roots were separated from shoots, spun in a low-speed centrifuge for 30 s to remove surface water, weighed, and counted for γ-ray emissions. A small subset of experiments were conducted, as above for the concentration-dependent isotherm, but with <sup>42</sup>K (half-life = 12.36 h; Coskun et al., 2013).

For compartmental analysis by tracer efflux, roots were exposed for 1 h in loading solution to maximize intracellular-specific activity of the tracer (Kronzucker et al., 1997), then placed in efflux funnels and eluted of radioactivity with successive 20-mL aliquots of fresh, nonlabeled growth solution for various washout periods. The desorption series was timed as follows, from first to final eluate: 1.5 min (twice), 1 min (nine times), for a total of 12 min. A subset of experiments involved either chemical (pH 7.25, 8.25, and 9.25 or complete NH<sub>3</sub>/NH<sub>4</sub><sup>+</sup> withdrawal) or cold (4°C) treatment for the final 5 min of elution (see “Results”). Another subset involved a longer elution protocol (30 min; Coskun et al., 2012) and the sudden (at 15 min) application of 500 μM AgNO<sub>3</sub> to disrupt membranes and release tracer accumulated in the cell (Coskun et al., 2012). Following elution, roots were handled as above, and radioactivity in roots, shoots, and efflux eluates were counted.

To quantify the chemical amount of released NH<sub>3</sub>/NH<sub>4</sub><sup>+</sup> during Ag<sup>+</sup> application (above), an integration technique was employed as described in detail elsewhere (Coskun et al., 2012). In brief, the summation of radioactivity released (in counts per min) during Ag<sup>+</sup> treatment was divided by the internal specific activity at the time of Ag<sup>+</sup> application (taking into account the exponential rise in specific activity during loading and its decline during elution up to the time of Ag<sup>+</sup> application) and corrected for root fresh weight.

### Electrophysiological Measurements

Membrane potential differences in epidermal and cortical root cells from intact barley seedlings were measured as described in detail elsewhere (Schulze et al., 2012). In brief, roots were immersed in growth solution in a plexiglass cuvette mounted onto a light microscope. Root cells were impaled with a glass micro-electrode, and potential differences were recorded with the use of an electrometer. Once stable readings were achieved, growth solution was exchanged by use of peristaltic pumps at approximately 7.5 mL min<sup>-1</sup>. Treatments included growth solution supplemented with rising concentrations of either NH<sub>3</sub>/NH<sub>4</sub><sup>+</sup> or K<sup>+</sup> (see “Results”), and ΔΔΨ<sub>m</sub> was recorded.

### Respiration Measurements

Root respiration was measured in intact barley seedlings as described in detail elsewhere (Malagoli et al., 2008). In brief, roots of 7-d-old seedlings were immersed in growth solution in a 3-mL Hansatech cuvette/O<sub>2</sub> electrode system, and the decline in dissolved O<sub>2</sub> was recorded over 10 min, after which roots were dried and weighed, as described above.

### Tissue Content Measurements

Tissue NH<sub>4</sub><sup>+</sup> content was determined by the OPA method as described in detail elsewhere (Coskun et al., 2012). Briefly, roots of 7-d-old intact seedlings were immersed for 5 min in aerated 10 mM CaSO<sub>4</sub> to desorb extracellular NH<sub>4</sub><sup>+</sup>, and plant organs were harvested as described above. For treatments, roots were first immersed for 15 min in aerated growth solution supplemented with either 500 μM AgNO<sub>3</sub>, 500 μM HgCl<sub>2</sub>, or pH 9.25 (titrated with NaOH) prior to CaSO<sub>4</sub> desorption. From there, root and shoot tissue was pulverized under liquid N<sub>2</sub>, and NH<sub>4</sub><sup>+</sup> was extracted with 10 mM formic acid (Husted et al., 2000). Purified supernatant was added to OPA reagent (Goyal et al., 1988; Coskun et al., 2012), and the color was left to develop in the dark at room temperature for 30 min. Sample absorbance was measured at 410 nm using a spectrophotometer.

### Supplemental Data

The following materials are available in the online version of this article.

**Supplemental Figure S1.** pH dependence of root <sup>13</sup>NH<sub>3</sub>/<sup>13</sup>NH<sub>4</sub><sup>+</sup> efflux and its relationship to influx.

## ACKNOWLEDGMENTS

We thank the team at the Canadian Association for Mental Health for providing  $^{13}\text{N}$ , the McMaster Nuclear Reactor team for providing  $^{42}\text{K}$ , and Jessie R. Wong for assistance with experiments.

Received July 31, 2013; accepted October 14, 2013; published October 17, 2013.

## LITERATURE CITED

- Amthor JS** (2000) The McCree-de Wit-Penning de Vries-Thornley respiration paradigms: 30 years later. *Ann Bot* **86**: 1–20
- Balkos KD, Britto DT, Kronzucker HJ** (2010) Optimization of ammonium acquisition and metabolism by potassium in rice (*Oryza sativa* L. cv. IR-72). *Plant Cell Environ* **33**: 23–34
- Barker AV, Maynard DN, Lachman WH** (1967) Induction of tomato stem and leaf lesions, and potassium deficiency, by excessive ammonium nutrition. *Soil Sci* **103**: 319–327
- Bobbink R, Hicks K, Galloway J, Spranger T, Alkemade R, Ashmore M, Bustamante M, Cinderby S, Davidson E, Dentener F, et al** (2010) Global assessment of nitrogen deposition effects on terrestrial plant diversity: a synthesis. *Ecol Appl* **20**: 30–59
- Bobbink R, Hornung M, Roelofs JG** (1998) The effects of air-borne nitrogen pollutants on species diversity in natural and semi-natural European vegetation. *J Ecol* **86**: 717–738
- Britto DT, Glass AD, Kronzucker HJ, Siddiqi MY** (2001a) Cytosolic concentrations and transmembrane fluxes of  $\text{NH}_4^+/\text{NH}_3$ . An evaluation of recent proposals. *Plant Physiol* **125**: 523–526
- Britto DT, Kronzucker HJ** (2002)  $\text{NH}_4^+$  toxicity in higher plants: a critical review. *J Plant Physiol* **159**: 567–584
- Britto DT, Kronzucker HJ** (2003) Trans-stimulation of  $^{15}\text{NH}_4^+$  efflux provides evidence for the cytosolic origin of tracer in the compartmental analysis of barley roots. *Funct Plant Biol* **30**: 1233–1238
- Britto DT, Kronzucker HJ** (2006) Futile cycling at the plasma membrane: a hallmark of low-affinity nutrient transport. *Trends Plant Sci* **11**: 529–534
- Britto DT, Kronzucker HJ** (2008) Cellular mechanisms of potassium transport in plants. *Physiol Plant* **133**: 637–650
- Britto DT, Kronzucker HJ** (2009) Ussing's conundrum and the search for transport mechanisms in plants. *New Phytol* **183**: 243–246
- Britto DT, Siddiqi MY, Glass AD, Kronzucker HJ** (2001b) Futile transmembrane  $\text{NH}_4^+$  cycling: a cellular hypothesis to explain ammonium toxicity in plants. *Proc Natl Acad Sci USA* **98**: 4255–4258
- Britto DT, Siddiqi MY, Glass ADM, Kronzucker HJ** (2002) Subcellular  $\text{NH}_4^+$  flux analysis in leaf segments of wheat (*Triticum aestivum*). *New Phytol* **155**: 373–380
- Chen G, Guo S, Kronzucker HJ, Shi W** (2013) Nitrogen use efficiency (NUE) in rice links to  $\text{NH}_4^+$  toxicity and futile  $\text{NH}_4^+$  cycling in roots. *Plant Soil* **369**: 351–363
- Coskun D, Britto DT, Jean YK, Schulze LM, Becker A, Kronzucker HJ** (2012) Silver ions disrupt  $\text{K}^+$  homeostasis and cellular integrity in intact barley (*Hordeum vulgare* L.) roots. *J Exp Bot* **63**: 151–162
- Coskun D, Britto DT, Kronzucker HJ** (2010) Regulation and mechanism of potassium release from barley roots: an in planta  $^{42}\text{K}^+$  analysis. *New Phytol* **188**: 1028–1038
- Coskun D, Britto DT, Li MY, Oh S, Kronzucker HJ** (2013) Capacity and plasticity of potassium channels and high-affinity transporters in roots of barley and Arabidopsis. *Plant Physiol* **162**: 496–511
- de Graaf MC, Bobbink R, Roelofs JG, Verbeek PJ** (1998) Differential effects of ammonium and nitrate on three heathland species. *Plant Ecol* **135**: 185–196
- Ehlert C, Maurel C, Tardieu F, Simonneau T** (2009) Aquaporin-mediated reduction in maize root hydraulic conductivity impacts cell turgor and leaf elongation even without changing transpiration. *Plant Physiol* **150**: 1093–1104
- Essah PA, Davenport R, Tester M** (2003) Sodium influx and accumulation in Arabidopsis. *Plant Physiol* **133**: 307–318
- Feng JN, Volk RJ, Jackson WA** (1994) Inward and outward transport of ammonium in roots of maize and sorghum: contrasting effects of methionine sulfoximine. *J Exp Bot* **45**: 429–439
- Fowler D, Coyle M, Skiba U, Sutton MA, Cape JN, Reis S, Sheppard LJ, Jenkins A, Grizzetti B, Galloway JN, et al** (2013) The global nitrogen cycle in the twenty-first century. *Philos Trans R Soc Lond B Biol Sci* **368**: 20130164
- Galloway JN, Townsend AR, Erismann JW, Bekunda M, Cai ZC, Freney JR, Martinelli LA, Seitzinger SP, Sutton MA** (2008) Transformation of the nitrogen cycle: recent trends, questions, and potential solutions. *Science* **320**: 889–892
- Gerendas J, Zhu ZJ, Bendixen R, Ratcliffe RG, Sattelmacher B** (1997) Physiological and biochemical processes related to ammonium toxicity in higher plants. *Z Pflanzen Bodenkd* **160**: 239–251
- Goyal SS, Rains DW, Huffaker RC** (1988) Determination of ammonium ion by fluorometry or spectrophotometry after on-line derivatization with *o*-phthalaldehyde. *Anal Chem* **60**: 175–179
- Gruber N, Galloway JN** (2008) An Earth-system perspective of the global nitrogen cycle. *Nature* **451**: 293–296
- Grzebisz W, Gransee A, Szczepaniak W, Diatta J** (2013) The effects of potassium fertilization on water-use efficiency in crop plants. *J Plant Nutr Soil Sci* **176**: 355–374
- Holm LM, Jahn TP, Möller AL, Schjoerring JK, Ferri D, Klaerke DA, Zeuthen T** (2005)  $\text{NH}_3$  and  $\text{NH}_4^+$  permeability in aquaporin-expressing *Xenopus* oocytes. *Pflügers Arch* **450**: 415–428
- Hove RM, Bhawe M** (2011) Plant aquaporins with non-aqua functions: deciphering the signature sequences. *Plant Mol Biol* **75**: 413–430
- Husted S, Hebborn CA, Mattsson M, Schjoerring JK** (2000) A critical experimental evaluation of methods for determination of  $\text{NH}_4^+$  in plant tissue, xylem sap and apoplastic fluid. *Physiol Plant* **109**: 167–179
- Izaurrealde R, Kissel D, Cabrera M** (1990) Simulation model of banded ammonia in soils. *Soil Sci Soc Am J* **54**: 917–922
- Jahn TP, Möller AL, Zeuthen T, Holm LM, Klaerke DA, Mohsin B, Kühlbrandt W, Schjoerring JK** (2004) Aquaporin homologues in plants and mammals transport ammonia. *FEBS Lett* **574**: 31–36
- Javot H, Lauvergeat V, Santoni V, Martin-Laurent F, Güçlü J, Vinh J, Heyes J, Franck KI, Schäffner AR, Bouchez D, et al** (2003) Role of a single aquaporin isoform in root water uptake. *Plant Cell* **15**: 509–522
- Kosegarten H, Grolig F, Esch A, Glusenkamp KH, Mengel K** (1999) Effects of  $\text{NH}_4^+$ ,  $\text{NO}_3^-$  and  $\text{HCO}_3^-$  on apoplast pH in the outer cortex of root zones of maize, as measured by the fluorescence ratio of fluorescein boronic acid. *Planta* **209**: 444–452
- Kosegarten H, Grolig F, Wieneke J, Wilson G, Hoffmann B** (1997) Differential ammonia-elicited changes of cytosolic pH in root hair cells of rice and maize as monitored by 2',7'-bis-(2-carboxyethyl)-5 (and -6)-carboxyfluorescein-fluorescence ratio. *Plant Physiol* **113**: 451–461
- Kozono D, Yasui M, King LS, Agre P** (2002) Aquaporin water channels: atomic structure molecular dynamics meet clinical medicine. *J Clin Invest* **109**: 1395–1399
- Kronzucker HJ, Britto DT** (2011) Sodium transport in plants: a critical review. *New Phytol* **189**: 54–81
- Kronzucker HJ, Siddiqi MY, Glass AD** (1996) Kinetics of  $\text{NH}_4^+$  influx in spruce. *Plant Physiol* **110**: 773–779
- Kronzucker HJ, Siddiqi MY, Glass AD** (1997) Conifer root discrimination against soil nitrate and the ecology of forest succession. *Nature* **385**: 59–61
- Kronzucker HJ, Szczerba MW, Britto DT** (2003) Cytosolic potassium homeostasis revisited:  $^{42}\text{K}$ -tracer analysis in *Hordeum vulgare* L. reveals set-point variations in  $\text{K}^+$ . *Planta* **217**: 540–546
- Kurimoto K, Day DA, Lambers H, Noguchi K** (2004) Effect of respiratory homeostasis on plant growth in cultivars of wheat and rice. *Plant Cell Environ* **27**: 853–862
- Lang B, Kaiser WM** (1994) Solute content and energy status of roots of barley plants cultivated at different pH on nitrate- or ammonium-nitrogen. *New Phytol* **128**: 451–459
- Lazof D, Cheeseman JM** (1986) Sodium transport and compartmentation in *Spergularia marina*: partial characterization of a functional symplasm. *Plant Physiol* **81**: 742–747
- Lee R, Ratcliffe RG** (1991) Observations on the subcellular distribution of the ammonium ion in maize root tissue using in-vivo  $^{14}\text{N}$ -nuclear magnetic resonance spectroscopy. *Planta* **183**: 359–367
- Lee RB, Ayling SM** (1993) The effect of methionine sulfoximine on the absorption of ammonium by maize and barley roots over short periods. *J Exp Bot* **44**: 53–63
- Lee RB, Clarkson DT** (1986) Nitrogen-13 studies of nitrate fluxes in barley roots. 1. Compartmental analysis from measurements of  $^{13}\text{N}$  efflux. *J Exp Bot* **37**: 1753–1767
- Loqué D, Ludewig U, Yuan L, von Wirén N** (2005) Tonoplast intrinsic proteins AtTIP2;1 and AtTIP2;3 facilitate  $\text{NH}_3$  transport into the vacuole. *Plant Physiol* **137**: 671–680
- Loqué D, von Wirén N** (2004) Regulatory levels for the transport of ammonium in plant roots. *J Exp Bot* **55**: 1293–1305



- Ludewig U, Neuhäuser B, Dynowski M (2007) Molecular mechanisms of ammonium transport and accumulation in plants. *FEBS Lett* **581**: 2301–2308
- Malagoli P, Britto DT, Schulze LM, Kronzucker HJ (2008) Futile Na<sup>+</sup> cycling at the root plasma membrane in rice (*Oryza sativa* L.): kinetics, energetics, and relationship to salinity tolerance. *J Exp Bot* **59**: 4109–4117
- Martre P, Morillon R, Barrieu F, North GB, Nobel PS, Chrispeels MJ (2002) Plasma membrane aquaporins play a significant role during recovery from water deficit. *Plant Physiol* **130**: 2101–2110
- Maurel C, Verdoucq L, Luu DT, Santoni V (2008) Plant aquaporins: membrane channels with multiple integrated functions. *Annu Rev Plant Biol* **59**: 595–624
- McClellan CJ, van den Berg LJ, Ashmore MR, Preston CD (2011) Atmospheric nitrogen deposition explains patterns of plant species loss. *Glob Change Biol* **17**: 2882–2892
- Morais-Cabral JH, Zhou YF, MacKinnon R (2001) Energetic optimization of ion conduction rate by the K<sup>+</sup> selectivity filter. *Nature* **414**: 37–42
- Pearson J, Stewart GR (1993) The deposition of atmospheric ammonia and its effects on plants. *New Phytol* **125**: 283–305
- Poorter H, Vanderwerf A, Atkin OK, Lambers H (1991) Respiratory energy requirements of roots vary with the potential growth rate of a plant species. *Physiol Plant* **83**: 469–475
- Rawat SR, Silim SN, Kronzucker HJ, Siddiqi MY, Glass AD (1999) AtAMT1 gene expression and NH<sub>4</sub><sup>+</sup> uptake in roots of *Arabidopsis thaliana*: evidence for regulation by root glutamine levels. *Plant J* **19**: 143–152
- Roberts JK, Wemmer D, Ray PM, Jandetzky O (1982) Regulation of cytoplasmic and vacuolar pH in maize root tips under different experimental conditions. *Plant Physiol* **69**: 1344–1347
- Saparov SM, Liu K, Agre P, Pohl P (2007) Fast and selective ammonia transport by aquaporin-8. *J Biol Chem* **282**: 5296–5301
- Scherer HW, Mackown CT, Leggett JE (1984) Potassium ammonium uptake interactions in tobacco seedlings. *J Exp Bot* **35**: 1060–1070
- Schulze LM, Britto DT, Li M, Kronzucker HJ (2012) A pharmacological analysis of high-affinity sodium transport in barley (*Hordeum vulgare* L.): a <sup>24</sup>Na<sup>+</sup>/<sup>42</sup>K<sup>+</sup> study. *J Exp Bot* **63**: 2479–2489
- Schuster E (1991) The behavior of mercury in the soil with special emphasis on complexation and adsorption processes: a review of the literature. *Water Air Soil Pollut* **56**: 667–680
- Stevens CJ, Dise NB, Mountford JO, Gowing DJ (2004) Impact of nitrogen deposition on the species richness of grasslands. *Science* **303**: 1876–1879
- Sweiry JH, Muñoz M, Mann GE (1991) Cis-inhibition and trans-stimulation of cationic amino acid transport in the perfused rat pancreas. *Am J Physiol* **261**: C506–C514
- Szczerba MW, Britto DT, Balkos KD, Kronzucker HJ (2008) Alleviation of rapid, futile ammonium cycling at the plasma membrane by potassium reveals K<sup>+</sup>-sensitive and -insensitive components of NH<sub>4</sub><sup>+</sup> transport. *J Exp Bot* **59**: 303–313
- ten Hoopen F, Cuin TA, Pedas P, Hegelund JN, Shabala S, Schjoerring JK, Jahn TP (2010) Competition between uptake of ammonium and potassium in barley and Arabidopsis roots: molecular mechanisms and physiological consequences. *J Exp Bot* **61**: 2303–2315
- Törnroth-Horsefield S, Wang Y, Hedfalk K, Johanson U, Karlsson M, Tajkhorshid E, Neutze R, Kjellbom P (2006) Structural mechanism of plant aquaporin gating. *Nature* **439**: 688–694
- Tournaire-Roux C, Sutka M, Javot H, Gout E, Gerbeau P, Luu DT, Bligny R, Maurel C (2003) Cytosolic pH regulates root water transport during anoxic stress through gating of aquaporins. *Nature* **425**: 393–397
- Vale FR, Volk RJ, Jackson WA (1988) Simultaneous influx of ammonium and potassium into maize roots: kinetics and interactions. *Planta* **173**: 424–431
- Van Beusichem ML, Kirkby EA, Baas R (1988) Influence of nitrate and ammonium nutrition on the uptake, assimilation, and distribution of nutrients in *Ricinus communis*. *Plant Physiol* **86**: 914–921
- Van Breemen N, Burrough PA, Velthorst EJ, Van Dobben HF, De Wit T, Ridder TB, Reijnders HF (1982) Soil acidification from atmospheric ammonium sulfate in forest canopy throughfall. *Nature* **299**: 548–550
- Vitousek PM, Aber JD, Howarth RW, Likens GE, Matson PA, Schindler DW, Schlesinger WH, Tilman D (1997) Human alteration of the global nitrogen cycle: sources and consequences. *Ecol Appl* **7**: 737–750
- von Wirén N, Gazzarrini S, Gojon A, Frommer WB (2000) The molecular physiology of ammonium uptake and retrieval. *Curr Opin Plant Biol* **3**: 254–261
- Walker DJ, Leigh RA, Miller AJ (1996) Potassium homeostasis in vacuolate plant cells. *Proc Natl Acad Sci USA* **93**: 10510–10514
- Wang MY, Siddiqi MY, Glass AD (1996) Interactions between K<sup>+</sup> and NH<sub>4</sub><sup>+</sup>: effects on ion uptake by rice roots. *Plant Cell Environ* **19**: 1037–1046
- Wang MY, Siddiqi MY, Ruth TJ, Glass AD (1993a) Ammonium uptake by rice roots. 1. Fluxes and subcellular distribution of <sup>15</sup>NH<sub>4</sub><sup>+</sup>. *Plant Physiol* **103**: 1249–1258
- Wang MY, Siddiqi MY, Ruth TJ, Glass AD (1993b) Ammonium uptake by rice roots. 2. Kinetics of <sup>15</sup>NH<sub>4</sub><sup>+</sup> influx across the plasmalemma. *Plant Physiol* **103**: 1259–1267
- Weise T, Kai M, Piechulla B (2013) Bacterial ammonia causes significant plant growth inhibition. *PLoS ONE* **8**: e63538
- Wells DM, Miller AJ (2000) Intracellular measurement of ammonium in *Chara corallina* using ion-selective microelectrodes. *Plant Soil* **221**: 103–106
- White MF, Christensen HN (1982) The 2-way flux of cationic amino acids across the plasma membrane of mammalian cells is largely explained by a single transport system. *J Biol Chem* **257**: 69–80